

التطور الجيوكيميائي والجيوفيزيائي لأنسياب الوشاح الأقليمي تحت الحرات البركانية

Geochemical and Geophysical Evolution of Regional Mantle Upwelling Beneath Volcanic Harrats

Summary

Our knowledge of the distribution, structure, composition and timing of the volcanic provinces (harrats) of western Saudi Arabia has been acquired from geological and geochemical studies since the 1970s. Complementary geophysical studies have produced information about lithospheric structure and plate kinematics. This previous work provides a solid context from which to pose detailed questions and hypotheses about regional scale mantle flow, volcanic activity and continental lithosphere modification, which can be answered or tested with new, high-resolution studies of the timing and composition of selected harrats, coupled with geophysical imaging of the crust and upper mantle beneath them. We propose a 2-year research program of combined field, geochronological, geochemical and geophysical studies in the western Arabian harrats volcanic province to evaluate these questions:

- What do the temporal, spatial and compositional variations in magmas that have penetrated the western Arabian shield tell us about modification of the continental lithosphere and upper mantle contributions to melting?
- What does the geodynamic origin of the volcanism predict about the longevity of crustal heat sources and mantle melting anomalies?
- Can we detect the influence of the Afar plume, which appears from seismic imaging to be channeled northward beneath the Arabian shield?
- If Afar mantle is not a significant influence, are other mantle plumes (upwelling from beneath the Arabian shield) important?

We will work with volcanic and upper mantle xenolithic samples provided by the US Geological Survey-Saudi Geological Survey regional mapping programs, the collections of several previous investigators, and our own fieldwork to fill in any gaps in coverage. Our analytical methods include ^{40}Ar - ^{39}Ar incremental heating age determinations, XRF and ICP-MS major, trace and rare earth element analyses, electron microprobe and laser

ablation ICP-MS for melt inclusion compositions, He and Ne isotopic analyses by mass spectrometry (all at Oregon State University), and arrays of broadband stations across the province to apply surface wave and receiver function analyses and interpretation of Moho and lithosphere-asthenosphere structure beneath the harrats (to be completed by Al-Amri).

Introduction

Extensive Cenozoic basaltic lava fields occur in the western part of the Arabian peninsula (Fig. 1a), erupted from N-S oriented volcanic centers and forming one of the largest alkali basalt provinces in the world (area: 180,000 km²). These young volcanic fields lie within 200 km of the NW-trending eastern margin of the Red Sea. Interestingly, there is no counterpart to these volcanic centers on the western margin (African plate) of the Red Sea. Likewise, topography is more elevated and rugged on the Arabian side, compared with the African side (Bohannon et al., 1989). In contrast to the tholeiitic basalts of the Red Sea, lava compositions in this province are olivine-transitional to alkali olivine-basalt to hawaiites, with minor more evolved compositions. Within several large centers, volcanic activity began (>12 Ma) with predominantly tholeiitic to transitional compositions, then became more alkalic for younger eruptions (<12 Ma). A prominent volcanic lineament, the N-S Makkah-Madinah-Nafud line, is the southward continuation of the Ha'il-Rutbah Arch axis of uplift of the Arabian shield (Fig. 1a), a Late Cretaceous-early Tertiary structure that was reactivated ~15 Ma. Hence flexure, extensional tectonics or asthenospheric flow could each explain the timing and distribution of the volcanic centers.

Mantle plumes have also been implicated in the western Arabia volcanism, anomalous topographic swells, continental breakup that formed the Red Sea and Gulf of Aden seafloor spreading systems and the voluminous flood basalts of Ethiopia and Yemen which are centered on the Afar region (Camp and Roobol, 1992; Daradich et al., 2003; Ebinger and Sleep, 1998; Schilling, 1973) (Fig. 1b). There is currently no consensus on the number of plumes and the geometry of associated mantle flow beneath East Africa and Arabia. Ebinger and Sleep (1998) propose that a single large plume may have caused multiple hotspots via channeled flow along thin lithosphere. This hypothesis

has been supported by a number of geophysical studies. For example, [Ritsema et al. \(1999\)](#) attribute the extensive volcanism around Afar to mantle flow from the African superplume, which is imaged beneath East Africa in their global S-velocity model. The regional travel time tomographic results of [Benoit et al. \(2006\)](#) support a single plume beneath Ethiopia. Numerical experiments by [Daradich et al. \(2003\)](#) suggest that rift-flank uplift along the Red Sea was induced by the African superplume. On the other hand, numerical mantle convection models of [Lin et al. \(2005\)](#) show that double-plume models can reproduce the distribution of East-African magmatism in space and time. Finite-frequency tomography ([Montelli et al., 2004](#)) shows that the Afar plume has a cylindrical, vertical tail through the lower mantle, separate from the African superplume. However, they do not rule out that the Afar plume may merge into the African superplume in the deep lower mantle. Shear-wave splitting and tomographic results of [Hansen et al. \(2006\)](#) and [Park et al. \(2007, 2008\)](#) suggest channeled horizontal mantle flow northward from the Afar hotspot.

Alternatively, several geochemical studies have proposed the existence of two distinct mantle plumes beneath East Africa. [George et al. \(1998\)](#) used $^{40}\text{Ar}/^{39}\text{Ar}$ ages to propose distinct mantle plumes beneath Afar and Kenya. [Nelson et al. \(2007, 2008\)](#) and [Rogers et al. \(2000\)](#) also assert two distinct mantle plumes based on Sr, Nd, and Pb isotope evidence. [Pik et al. \(2006\)](#) used $^3\text{He}/^4\text{He}$ ratios to suggest that a unique large mantle plume could not feed all the Cenozoic African volcanic provinces. [Camp and Roobol \(1992\)](#) question whether one Afar plume can feed widespread volcanism over a distance of 2000 km, and suggest that the western Arabian volcanic activity is due to an independent plume arising beneath the Arabian shield. [Furman et al. \(2006\)](#) present geochemical evidence that suggests these different plumes could all stem from a common large mantle plume such as the African superplume.

Project Objectives

The proposed research will apply geochronological and petrochemical methods to selected centers in the harrats volcanic province to determine the time and space relations of the erupted magmas, the compositional nature of mantle sources and the conditions of partial melting beneath western Saudi Arabia. Geophysical studies of the crust and upper

mantle beneath the volcanic areas will image the crustal structure and lithosphere-asthenosphere boundary, and provide data to evaluate the extent of magmatic modification of the continental lithosphere.

The data acquired will be directed at answering these regional questions:

1. What do the temporal, spatial and compositional variations in magmas that have penetrated the western Arabian shield tell us about modification of the continental lithosphere and upper mantle contributions to melting?
2. What does the geodynamic origin of the volcanism predict about the longevity of crustal heat sources and mantle melting anomalies?
3. Can we detect the influence of the Afar plume, which appears from seismic imaging to be channeled northward beneath the Arabian shield?
4. If Afar mantle is not a significant influence, are other mantle plumes (upwelling from beneath the Arabian shield) important?

Background and Literature Review

Two distinct phases of continental magmatism are evident in western Saudi Arabia (Fig. 2, 3). The first, erupted from about 30 to 20 Ma, produced tholeiitic-to-transitional lavas emplaced along NW trends. The second, from about 12 Ma to present, produced transitional-to-strongly-alkalic lavas emplaced along N-S trends. The older phase, predominantly dikes and smaller centers proximal to the Red Sea, is attributed to passive-mantle upwelling during extension of the Red Sea basin, whereas the younger phase is attributed to active-mantle upwelling facilitated by minor continental extension perpendicular to plate collision (Hempton, 1987). The younger magmatic phase is largely contemporaneous with a major period of crustal uplift that produced the west Arabian Swell after about 14 Ma. A variety of evidence suggests that the west Arabian Swell is thermally supported by hot, upwelling asthenosphere. In contrast to the distinct asymmetry of uplift and magmatism on opposing sides of the Red Sea basin, these processes were symmetric across a N-S line marking the central axis of the west Arabian Swell. This axis coincides with two fundamental features: the Ha'il-Rutbah Arch in the north, and the Makkah-Madinah-Nafud (MMN) volcanic line in the south. The symmetry

of magmatism is demonstrated by petrochemical evidence that the MMN harrats were derived by greater degrees of partial melting at shallower depths than those harrats lying to the west and east of the MMN line. The potential temperature of the asthenosphere is estimated to be about $\sim 100^{\circ}\text{C}$ greater beneath the MMN line than beneath the flanking, more undersaturated harrats (Camp and Roobol, 1992).

Major and trace element compositions of the harrat volcanic rocks provide evidence for variable depth and degree of partial melting of the mantle beneath the west Arabian Swell. The harrats forming the MMN line were produced by greater total degrees of melting over a more extensive depth range of melting, compared with harrats east and west of the N-S axis that resulted from deeper melt separation and smaller degrees of mantle melting. Evidence of this general pattern comes from trace element compositions that are sensitive to melting conditions (Fig. 4). For example, the degree of partial melting from a peridotite source should be reflected in the Zr/Nb ratios of the derivative lavas. The distribution coefficient for Zr in clinopyroxene is about 10 times larger than that for Nb, so higher Zr/Nb ratios indicate greater degrees of partial melting from mantle peridotite (Altherr et al., 1988). From 68 representative harrat samples from Saudi Arabia, Altherr et al. (1990) demonstrate that the largest Zr/Nb ratios are from the MMN line (Harrat Rahat) and that the smallest ratios are from harrats located the farthest to the west (Uwayrid) and east (Hutaymah) of the MMN line. Although there is little evidence for a systematic variation in these reconnaissance data, it is clear (Fig. 4) that the MMN lavas have significantly higher Zr/Nb ratios reflecting overall greater degrees of partial melting than Zr/Nb values for the more alkalic lavas from Harrat Kura to the west and Harrat Kishb to the east. New data from Harrat Lunayyir (Al-Amri et al., unpublished) fall within the range of Harrat Kishb data and confirm the E-W pattern of Zr/Nb. What is missing is any knowledge of how melt compositions may have changed with time (12 Ma to present) across the region.

Various isotopic tracers (e.g., Sr, Nd, Pb) have traditionally been used to identify the contributions of potential source rocks (PreCambrian crust, continental lithosphere, asthenosphere, mantle plume) to continental volcanic provinces. Altherr et al. (1990) conclude that such isotopic data indicate that harrat lavas have formed from melting of lithospheric mantle and asthenosphere, with very little crustal contribution. This agrees

with evidence from mantle xenoliths carried to the surface in harrat lavas, that the asthenosphere-lithosphere boundary under the region is about 60 km deep – considerably shallower than for unmodified continental shield, and hence compatible with significant lithospheric thinning by thermal erosion (McGuire, 1988a). Helium and neon isotopes are ideal tracers to quantify contributions of mantle plumes, which are characterized by a higher proportion of primordial solar-type noble gases compared to lithospheric or asthenospheric mantle sources. Hopp et al. (2003) use such tracers to investigate the role of the Afar mantle plume (a high $^3\text{He}/^4\text{He}$ plume of up to 20 R_A ; 1 R_A = atmospheric composition) during continental breakup of the Red Sea rift. They analyzed ultramafic rocks from Zabargad Island and mantle xenoliths from the Quaternary volcanic fields of Al Birk and Jizan (SW Saudi Arabia) that are representative of the local subcontinental lithospheric mantle. $^3\text{He}/^4\text{He}$ ratios range from 6.1 to 8.3 R_A , similar to results of worldwide lithospheric and asthenospheric mantle, and therefore are not indicative of a plume component. In contrast, they observe significant contributions of plume-derived neon, which is characterized by a higher proportion of primordial solar-type neon than typical mid-ocean ridge basalts (MORB).

Considering both helium and neon isotope systematics reveals mixing of a deep mantle plume, a pre-rift MORB-like, and a more radiogenic pre-rift lithospheric mantle component. As the deep mantle plume component has a higher Ne/He ratio when compared to the shallow mantle components, it is more prominent in Ne than in He, with up to 57% plume-derived neon and 11% plume-derived helium present in the investigated samples (Fig. 5). This study demonstrates that the Afar plume source contributed primordial noble gases to an intrinsically more radiogenic and nucleogenic lithospheric and asthenospheric component up to a distance of ~1800 km (Zabargad), even in the early stages of continental rifting, ~20 Ma. These results present the first unambiguous geochemical evidence suggesting an active role for the Afar mantle plume during the evolution of the Red Sea rift, supporting geochronological and geodynamic evidence. We expect that high-precision He and Ne measurements for olivine-bearing lavas and ultramafic xenoliths from the harrats (e.g., Uwayrid, Hutaymah, Kishb; Thornber, 1990, Vaughan, 1985; McGuire, 1988b; Ghent et al, 1980) will be similarly useful in quantifying contributions to melting from plume, lithosphere and asthenosphere mantle in

western Saudi Arabia.

Finally, geophysical methods (seismic, magnetics, heat flow) provide images of the crust and upper mantle beneath the western Arabian shield, which must relate closely to the dynamic history of mantle flow, lithospheric uplift, and volcanic activity. Regional structure is known from seismic refraction studies (Healy et al., 1982; Mooney et al., 1985; Gettings et al., 1986; Prodehl, 1986) and body and surface waves (Benoti et al., 2003; Julia et al., 2003). Additional information about upper mantle flow beneath the region comes from seismic anisotropy studies (Hansen et al, 2006, 2007). Recently, Chang and van der Lee (2011) report jointly inverted teleseismic S- and SKS-arrival times, regional S- and Rayleigh waveform fits, fundamental-mode Rayleigh-wave group velocities, and independent Moho constraints that provide complementary resolution for the three-dimensional (3-D) S-velocity structure beneath East Africa and Arabia. Their tomographic results help reconcile some of the competing explanations for the region's volcanism, uplift, and rifting.

Specifically, Chang and van der Lee (2011) find two distinct low-velocity anomalies, likely representing mantle plumes, beneath Afar and northern Kenya, which extend down to at least 1400 km depth (Fig. 6, 7). Extensive low-velocity anomalies in the uppermost mantle along with the shear-wave splitting results suggest horizontal mantle flow radially away from Afar. This radial flow seems to be organized in channels, potentially following thin lithosphere. One such channel follows the Gulf of Aden, supporting the notion of eastward-channeled mantle flow from Afar – this is confirmed by geochemical gradients identified from dredged rocks samples from the spreading ridge. Another channel extends northward beneath the southern Red Sea, but rather than extending to the central Red Sea, it continues northwards beneath western Saudi Arabia. A separate quasi-vertical low-velocity anomaly is found beneath Jordan and northern Arabia, likely representing a separate plume that may be responsible for the Karacalidag volcanic province in southern Turkey, Harrat Shamah in Jordan and Harrat Uwayrid in northern Saudi Arabia (Fig. 1a). This low-velocity anomaly extends significantly into the lower mantle, supporting geochemical evidence (Ilani et al., 2001) that the Neogene volcanism in Jordan has a deep mantle origin. This mantle plume may have contributed, along with the Afar plume, to the widespread volcanism and uplift in western Arabia.

The lava field of Harrat Lunayyir, on the western edge of the central portion of the N-S trend (west of Khaybar, Fig. 1a), has been selected for high-resolution age, composition and geophysical investigation by Al-Amri and Duncan (KSU). This study was initiated because Harrat Lunayyir experienced multiple seismic swarms since 2007. Recent studies (e.g. Pallister et al., 2010) have indicated that these swarms are associated with magma that has risen to shallow levels beneath Harrat Lunayyir, potentially increasing the likelihood of a volcanic eruption. It is estimated that at least twenty-one different eruptions have occurred in western Arabia over the past 1500 years (Camp et al., 1987), including one near Harrat Lunayyir about 1000 years ago. New age determinations by the ^{40}Ar - ^{39}Ar incremental heating method detail the volcanic history, which is generally younger than previously thought. That is, eruptions occurred within the Quaternary period, beginning about 0.6 Ma, and increased in frequency into historic times. Primitive and evolved lavas were erupted throughout the volcanic history, with no apparent trend in degree of crystal fractionation. However, the common occurrence of evolved compositions throughout the volcanic history indicates the significant role of a shallow level crustal magma chamber (Fig. 8, 9). Trace element ratios from Harrat Lunayyir lavas (Fig. 8), are compatible with variations in depth and degree of mantle melting such that centers near the axis were derived from shallower and more extensive melting, while centers at the margins were derived by deeper and less extensive melting (Fig. 10).

Project Design and Methodology

We have designed three complementary research themes to accomplish the project objectives:

1. Geochronology. Samples of previously mapped units in the volcanic stratigraphy of several selected harrats (Lunayyir, Kura, Khaybar, Ithnayn and Hutaymah, Fig. 1a) will be dated by the ^{40}Ar - ^{39}Ar incremental heating method to determine the time frame of activity. This method is both more accurate and has higher precision than the K-Ar method (by which the previous ages were determined) in its ability to identify and eliminate the effects of ^{40}Ar -loss and mantle-derived (“excess”) Ar. Additionally, new

generation multi-collector mass spectrometers have superior sensitivity, small and clean extraction lines, and resolution – allowing smaller amounts of radiogenic ^{40}Ar to be resolved; hence younger age limits. Preliminary data, for example, indicate that lavas at Harrat Lunayyir are significantly younger than previously estimated. New ages will be measured at Oregon State University using an MAP 215/50 mass spectrometer equipped with a single ion multiplier operated in peak-hopping mode, and a newly commissioned ARGUS VI five-collector mass spectrometer. Ages will be combined with unit volume estimates (from US Geological Survey-Saudi Geological Survey mapping) to obtain eruption rates throughout the volcanic history. Such age data will provide information about frequency of eruptions, and whether volcanic intensity is building or waning at each center. An important broader impact of this knowledge will be in the evaluation of the geothermal energy potential of several individual harrats (see Utilization of Results below).

[Camp and Roobol \(1992\)](#) recognize a progression in the age of *initial* volcanic activity (decreasing to the north) among harrats that define the MMN (i.e., Rahat [10 Ma], Khaybar [5 Ma], Ithnayn [3 Ma]). This trend could reflect northward flow of an asthenospheric source (Afar plume, Fig. 1b) and needs to be confirmed by dating the lowermost lava flows at each of these centers with modern methods. Age progressions among the initial lavas erupted, from one center to the next, can potentially distinguish one plume from multiple plumes (Figs. 1b, 7). Superior age data are also required to provide a time frame for geochemical variations within the province.

2. Geochemistry. Major and trace element compositions (determined by XRF and ICP-MS methods) will be used to document variability in parental magmas through time and space within the province. Specifically, samples from an E-W transect of volcanic centers (Hutaymah, Ithnayn, Khaybar, Kura and Lunayyir) will be examined for evidence of depth and degree of mantle melting, in order to test the proposed ([Camp and Roobol, 1992](#)) modification of the lithosphere/asthenosphere boundary beneath the region (Fig. 10). We will use major element compositions to establish pressure and temperature conditions, and degree of melting, using the approach pioneered by [McKenzie and Bickle \(1988\)](#) based on the experimental petrology database. We will use trace element

compositions to determine depth and extent of melting (e.g., Zr/Nb, La/Yb), following the strategy of [Fram and Leshner \(1993\)](#). We will also evaluate crustal magma chamber processes (e.g., crystal fractionation, crustal assimilation, magma recharge) using major and trace element chemistry as well as analyses of individual mineral phases.

In addition the melt inclusions in early formed phenocrysts (olivine and pyroxene) and potentially also in mantle xenoliths common in many of the centers (e.g., Hutaymah), will be determined using electron microprobe and ICP-MS laser ablation methods to identify the composition of primary melts, formed in the melting zone before homogenization of discrete melts into parental magmas (e.g. Kent et al., 2002, Kent, 2008). Using the noble gas laboratory at Oregon State University, equipped with a Nu Instruments Noblesse mass spectrometer, we will perform isotopic analyses (He, Ne) on selected samples of ultramafic xenoliths, and olivine-bearing lavas, to distinguish mantle sources for harrat volcanoes. In particular, these data will be used to evaluate asthenospheric, Afar mantle plume, or sub-continental Arabian shield mantle as potential contributors to melting that produced harrat volcanism.

3. Geophysics. We will investigate the velocity structure beneath Harrat Lunayyir using seismic travel-time tomography. In this method, absolute and relative travel-times from local and regional earthquakes are inverted for improved event relocations and models of seismic velocity structure. These data will allow us to delineate magmatic features, such as magma pathways, and seismic structures beneath the harrats, thereby giving us considerable information about the three-dimensional structure and modification of the Arabian shield crustal rocks.

We will investigate the crustal and upper mantle velocity structure beneath Harrat Lunayyir using body wave travel-time tomography. A number of different earthquake tomography packages are available, such as SIMULPS ([Thurber, 1983](#); [Thurber and Eberhart-Phillips, 1999](#); [Hansen et al., 2004](#)) and tomoDD ([Zhang and Thurber, 2003](#); [Pesicek et al., 2010](#)), which invert absolute and relative travel-times from local and regional earthquakes for improved event relocations and models of seismic velocity structure. Seismic velocity in a given region depends on the rock characteristics, such as porosity, fracturing, and fluid saturation, and its physical condition, such as temperature

and pressure. In volcanic environments, such as Harrat Lunayyir, the presence of fluids, cracks, and gas can also change the elastic properties (Mavko, 1980; Sato et al., 1989; Sanders et al., 1995). Figure 11 shows an example from Kilauea Volcano in Hawaii, where Hansen et al. (2004) used the travel-time tomography approach to relocate seismic events and determine the velocity structure beneath the south flank of the volcano. In Harrat Lunayyir, tomographic velocity variations determined with this approach will allow us to differentiate between the slow seismic velocities associated with magmatic features and the fast seismic velocities in the surrounding regions, thereby giving us considerable information about the three-dimensional structure. Additionally, the accurate earthquake locations determined as part of the tomographic analysis will help delineate the seismic structures in the crust beneath the harrats.

References

- Almond, D.C., 1986a. The relation of Mesozoic-Cainozoic volcanism to tectonics in the Afro-Arabian dome. *J. Volcanol. Geotherm. Res.*, 28: 225-246.
- Almond, D.C., 1986b. Geological evolution of the Afro-Arabian dome, *Tectonophysics*, 31: 301-332.
- Altherr, R., F. Henjes-Kunst, H. Puchelt and A. Baumann, 1988. Volcanic activity in the Red Sea axial trough—Evidence for a large mantle diapir. *Tectonophysics*, 150: 121-133.
- Altherr, R., F. Henjes-Kunst and A. Baumann, 1990. Asthenosphere versus lithosphere as possible sources for basaltic magmas erupted during formation of the Red Sea: Constraints from Sr, Pb and Nd isotopes. *Earth Planet. Sci. Lett.*, 96: 269-286.
- Arno, V., et al., 1980a. Recent volcanism within the Arabian plate: Preliminary data from Harrats Hadan and Nawasif-Al Buqum, in *Geodynamic Evolution of the Afro-Arabian Rift System*, Publ. 47, pp. 629-643, Academia Nazionale dei Lincei, Rome.
- Arno, V., et al., 1980b. Recent basic volcanism along the Red Sea coast: the Al Birk volcanic field in Saudi Arabia, in *Geodynamic evolution of the Afro-Arabian rift system*, Publ. 47, pp. 644-654, Academia Nazionale dei Lincei, Rome.
- Benoti, M.H., Nyblade, A.A., VanDecar, J.C. and Gurrola, H. 2003. Upper mantle P wave velocity structure and transition zone thickness beneath the Arabian Shield. *Geophys. Res. Lett.* 30: 1-4.
- Berthier, F., Damange, J., Lundt, R. and Verzier, P. 1981. Geothermal resources of the Kingdom of Saudi Arabia: Saudi Arabian Deputy Ministry for Mineral Resources Open File Rep. BRGM-OF-01-24, 112p.
- Bohannon, R.G., C.W. Naeser, D.L. Schmidt, and R.A. Zimmermann, 1989. The timing of uplift, volcanism and rifting peripheral to the Red Sea: A case for passive rifting? *J. Geophys. Res.*, 94: 1683-1701.
- Bonatti, E., 1985. Punctiform initiation of seafloor spreading in the Red Sea during transition from a continental to an oceanic rift. *Nature*, 316: 33-37.

- Camp, V .E., and M.J. Roobol, 1989. The Arabian continental alkali basalt province, Part I, Evolution of Harrat Rahat, Kingdom of Saudi Arabia. *Geol. Soc. Am. Bull.*, 101: 71-95.
- Camp, V .E., and M .J. Roobol, 1991. Comment on "Topographic and volcanic asymmetry around the Red Sea: Constraints on Red Sea models" by T.H. Dixon, E.R. Ivins and B.J. Franklin. *Tectonics*, 10: 649-652.
- Camp, V.E. and Roobol, M.J., 1991, Geologic Map of the Cenozoic Lava Field of Harrat Rahat, Kingdom of Saudi Arabia: Saudi Arabian Directorate General of Mineral Resources Geoscience Map GM-1233, scale 1:250,000 with text 37p.
- Camp, V.E., and Roobol, M.J., 1992, Upwelling asthenosphere beneath western Arabia and its regional implications: *Journal Geophysical Research*, v. 97, p.15,255-15,271.
- Camp, V.E., Hooper,P.R., Roobol, M.J. and White, D.L., 1987, The Madinah eruption, Saudi Arabia: Magma mixing and simultaneous extrusion of three basaltic chemical types: *Bulletin Volcanology*, v. 49, p.489-508.
- Camp, V.E., Roobol, V.E. and Hooper, P.R., 1989a, The Arabian continental alkali basalt province: Part I. Evolution of Harrat Rahat, Kingdom of Saudi Arabia: *Bulletin, Geological Society of America*, v. 101, p. 71-95.
- Camp, V.E., Roobol, M.J. and Hooper, P.R., 1991, The Arabian continental alkali basalt province: Part II. Evolution of Harrats Khaybar, Ithnayn, and Kura, Kingdom of Saudi Arabia: *Bulletin, Geological Society of America*, v. 103, p.363-391.
- Camp, V.E., Roobol, M.J., and Hooper, P.R., 1992, The Arabian continental alkali basalt province: Part III. Evolution of Harrat Kishb, Kingdom of Saudi Arabia: *Bulletin, Geological Society of America*, v. 104, p. 379-396.
- Chang, S.-J. and van der Lee, S., 2011. Mantle plumes and associated flow beneath Arabia and East Africa., *Earth Planet. Sci. Lett.*, 302: 448-454.
- Coleman, R.G., Fleck, R.J., Hedge, C.E. and Ghent, E.D., 1977. The volcanic rocks of southwest Saudi Arabia and the opening of the Red Sea, in *Red Sea research 1970-1975: Saudi Arabian Directorate General of Mineral resources Bull.* 22, p. D1-30.
- Coleman, R .G., and A.V. McGuire, 1988. Magma systems related to the Red Sea opening. *Tectonophysics*, 150: 77-100.
- Daradich, A., Mitrovica, J.X., Pysklywec, R.N, Willett, S.D. and Forte, A.M. (2003). Mantle flow, dynamic topography, and rift-flank uplift to Arabian. *Geol. Soc. Am.* 31:901-904.
- Dixon, T.H., E.R. Ivins, and B.J. Franklin, 1989. Topographic and volcanic asymmetry around the Red Sea: Constraints on rift models. *Tectonics*, 8: 1193-1216.
- Ebinger, C.J. and Sleep, N.H., 1998. Cenozoic magmatism throughout east Africa resulting from impact of a single plume. *Nature*, 395: 788-791.
- Fram, M.S. and Leshner, C.E., 1993. Geochemical constraints on mantle melting during creation of the North Atlantic basin. *Nature*, 363: 712-715.
- Furman, T., et al., 2006. Heads and tails: 30 million years of the Afar plume. In: Yirgu, G., Ebinger, C. and Maguire, P. (eds), *The Afar volcanic province within the East African Rift System. Geol. Soc. Spec. Publ.* 259: 95-119.
- Gettings, M. E., H.R. Blank, W.D. Mooney, and J.H. Healey, 1986. Crustal structure of southwestern Saudi Arabia, *J. Geophys. Res.*, 91: 6491- 6512.
- Ghent, E.D., Coleman, R.G. and Hadley, D.G., 1980. Ultramafic inclusions and host alkali olivine basalts of the southern coastal plain of the Red Sea, Saudi Arabia.

- Amer. J. Science, 280A: 499-527.
- Girdler, R.W. and Styles, P., 1974. Two stage Red Sea floor spreading. *Nature*, 247: 7-11.
- Girdler, R.W., 1978. Seafloor spreading in the western Gulf of Aden. *Nature*, 271: 615-617.
- Greenwood, W.R., 1973. The Ha'il arch--a key to the deformation of the Arabian Shield during evolution of the Red Sea rift. *Saudi Arabian Dir. Gen. Miner. Resource Bull.* 7: 5.
- Hansen, S., Thurber, C., Mandernach, M., Haslinger, F., and Doran, C., Seismic velocity and attenuation structure of the East Rift Zone and South Flank of Kilauea Volcano, Hawaii. *Bull. Seism. Soc. Am.*, 94, 1430-1440, 2004.
- Hansen, S., Schwartz, S., Al-Amri, A. and Rodgers, A., 2006. Combined plate motion and density driven flow in the asthenosphere beneath Saudi Arabia: evidence from shear-wave splitting and seismic anisotropy. *Geology*, V. 34, no. 10, p. 869 – 872.
- Hansen, S., Rodgers, A., Schwartz, S., and Al-Amri, A., 2007. Imaging ruptured lithosphere beneath the Red Sea and Arabian Peninsula. *Earth and Planet. Sci. Letters*, 259: 256 – 265.
- Healy, J.H., Mooney, W.D., Blank, H.R., Gettings, M.E., Kohler, W.M., Lamson, R.J. and Leone, L.E., 1982. Saudi Arabian seismic deep-refraction profile: Final project report, Ministry of Petroleum and Mineral Resources, Deputy Ministry for Mineral Resources, Kingdom of Saudi Arabia, Open File Report USGS-OF-02-37, 141 p.
- Hempton, M.R., 1987. Constraints on Arabian plate motion and extensional history of the Red Sea. *Tectonics* 6: 687-705.
- Henjes-Kunst F., R. Altherr, and A. Baumann, 1990. Evolution and composition of the lithospheric mantle underneath the western Arabian peninsula: Constraints from Sr-Nd isotope systematics of mantle xenoliths. *Contrib. Mineral. Petrol.*, 105: 460-472.
- Hill, R.I., 1991. Starting plumes and continental breakup. *Earth Planet. Sci. Lett.*, 104: 398-416.
- Hill, R.I., Campbell, I.H., Davies, G.F. and Griffiths, R.W., 1992. Mantle plumes and continental tectonics. *Science*, 256: 186-193.
- Hopp, J., Tieloff, M. and Altherr, R., 2004. Neon isotopes in mantle rocks from the Red Sea region reveal large-scale plume-lithosphere interaction. *Earth Planet. Sci. Lett.*, 219: 61-76.
- Jónsson, S.; Pallister, J.; McCausland, W., and El-Hadidy, S., 2010. Dyke Intrusion and Arrest in Harrat Lunayyir, western Saudi Arabia, in April-July 2009. *Geophysical Research Abstracts*, Vol. 12, EGU2010-7704.32 p.
- Julia, J., Ammon, C. and Herrmann, R., 2003. Lithosphere structure of the Arabian Shield from the joint inversion of receiver functions and surface-wave group velocities. *Tectonophysics* 371:1-21.
- Kuo, L.-C. and Essene, E.J., 1986. Petrology of spinel harzburgite xenoliths from the Kishb plateau, Saudi Arabia. *Contrib. Mineral. Petrol.*, 93: 335-346.
- McGuire, A.V., 1988a. Petrology of mantle xenoliths from Harrat al Kishb: The mantle beneath western Saudi Arabia. *J. Petrol.*, 29: 73-92.
- McGuire, A.V., 1988b. The mantle beneath the Red Sea margin: Xenoliths from western Saudi Arabia. *Tectonophysics*, 150: 101-119.
- McKenzie D. and M. J. Bickle, 1988. The volume and composition of melt generated by

- extension of the lithosphere. *J. Petrol.*, 29: 625-679.
- Mooney, W.D., Gettings, M.E., Blank, H.R. and Healy, J.W., 1985. Saudi Arabian seismic deep refraction profile: A travel-time interpretation of crust and upper mantle structure. *Tectonophysics*, 111: 173-246.
- Moufti, M.R.H. and Hashad, M.H., 2005. Volcanic hazards assessment of Saudi Arabian Harrats: geochemical and isotopic studies of selected areas of active Makkah-Madinah-Nafud (MMN) volcanic rocks. Final Project Report (LGP-5-27), King Abdulaziz City for Science and Technology, Riyadh, Saudi Arabia.
- Pallister, J. S., 1984. Reconnaissance geologic map of the Harrat Hutaymah quadrangle sheet 26/42A, Kingdom of Saudi Arabia, U.S. Geol. Surv. Open File Rep. USGS-OF-04-467, 7 pp.
- Pallister, J.S., 1987. Magmatic history of Red Sea rifting: Perspective from the central Saudi Arabian coastal plain. *Geol. Soc. Amer. Bull.*, 98: 400-417.
- Pallister, J.S., et al., 2010. Broad accommodation of rift-related extension recorded by dyke intrusion in Saudi Arabia. *Nature Geoscience*, DOI: 10.1038/NGE0966.
- Pesicek, J.D., Thurber, C.H., Zhang, H., DeShon, H.R., Engdahl, E.R., and Widiyantoro, S., 2010. Teleseismic double-difference relocation of earthquakes along the Sumatra-Andaman subduction zone using a three-dimensional model, *J. Geophys. Res.*, 115, doi: 10.1029/2010JB007443, 2010.
- Prodehl, C., 1986. Interpretation of a seismic-refraction survey across the Aravian Shield in western Saudi Arabia. *Tectonophysics*, 111: 247-282.
- Richards, M.A., Duncan, R.A. and Courtillot, V. E., 1989. Flood basalts and hot-spot tracks plume heads and tails. *Science*, 246: 103-107.
- Roobol, M.J. and Camp, V.E., 1991a, Geologic map of the Cenozoic Lava Fields of Harrats Khaybar, Ithnayn and Kura, Kingdom of Saudi Arabia: Saudi Arabian Directorate General of Mineral Resources Geoscience Map GH-131, scale 1:250,000 with text 40p.
- Roobol, M.J. and Camp, V.E., 1991b, Geologic map of the Cenozoic Lava Field of Harrat Kishb, Kingdom of Saudi Arabia: Saudi Arabian Directorate General of Mineral Resources Geoscience Map GM-132, scale 1:250,000 with text 34p.
- Schilling, J.-G., 1973. Afar mantle plume: Rare earth evidence. *Nature*, 242: 2-6.
- Styles, P. and Hall, S.A., 1980. A comparison of the seafloor spreading histories of the western Gulf of Aden and the central Red Sea, in geodynamic evolution of the Afro-Arabian rift system, Rome, Italy, *Accademia Nazionale dei Lincei*, p. 585-606.
- Thornber, C.R., 1990. Geologic map of Harrat Hutaymah, with petrologic classification and distribution of ultramafic inclusions, Saudi Arabia. U.S. Geol. Surv. Misc. Field Stud. Map, MF-2129, 1:100,000-scale.
- Thornber, C.R., and J.S. Pallister, 1985. Mantle xenoliths from northern Saudi Arabia. *Eos Trans. AGU*, 66: 393.
- Thurber, C., Earthquake locations and three-dimensional crustal structure in the Coyote Lake area, central California, *J. Geophys. Res.*, 88, 8226-8236, 1983.
- Thurber, C., and Eberhart-Phillips, D., Local earthquake tomography with flexible gridding, *Comp. Geosci.*, 25, 809-818, 1999.
- Vaughan, A.W., 1985. Mantle xenoliths from Harrat al Kishb, western Saudi Arabia. *EOS, Trans. Amer. Geophys. Union*, 66: 1114.

Figures

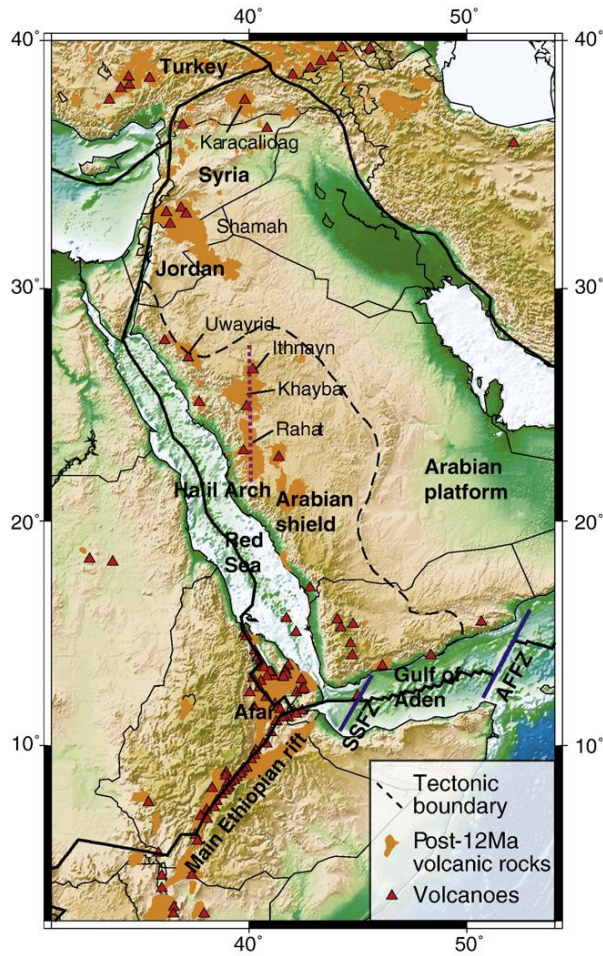


Figure 1a. Topographic map for Arabia and northeastern Africa. Volcanoes and post-12 Ma volcanic rocks are indicated by red triangles and orange area, respectively. Thick solid lines indicate plate boundaries. A dotted purple line represents the Ha'il Rutbah Arch and MMN lineament. SSFZ: Shukra El Sheik Fracture zone; AFFZ: Alula Fartak Fracture zone. From [Chang and van der Lee \(2011\)](#).

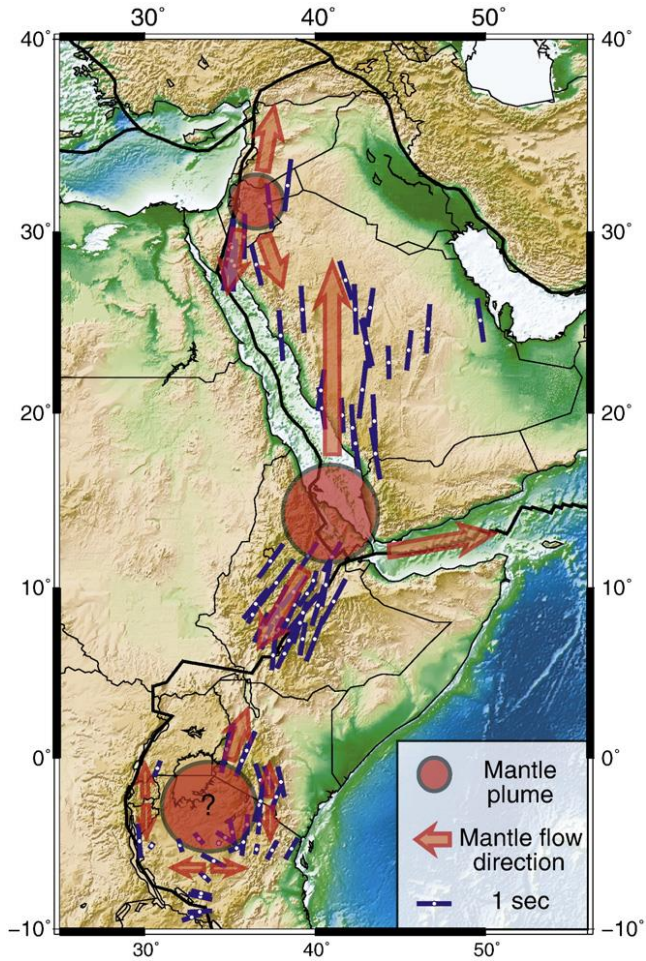


Figure 1b. Schematic map which shows locations of proposed mantle plumes and mantle flow directions along with fast axes of shear-wave splitting [Hansen et al. (2006), and Walker et al.(2004)]. The locations of the Afar and Jordan plumes are from the 150 km depth slice in Fig. 10. The location of the Kenya plume is based on Weeraratne et al. (2003). From Chang and van der Lee (2011).

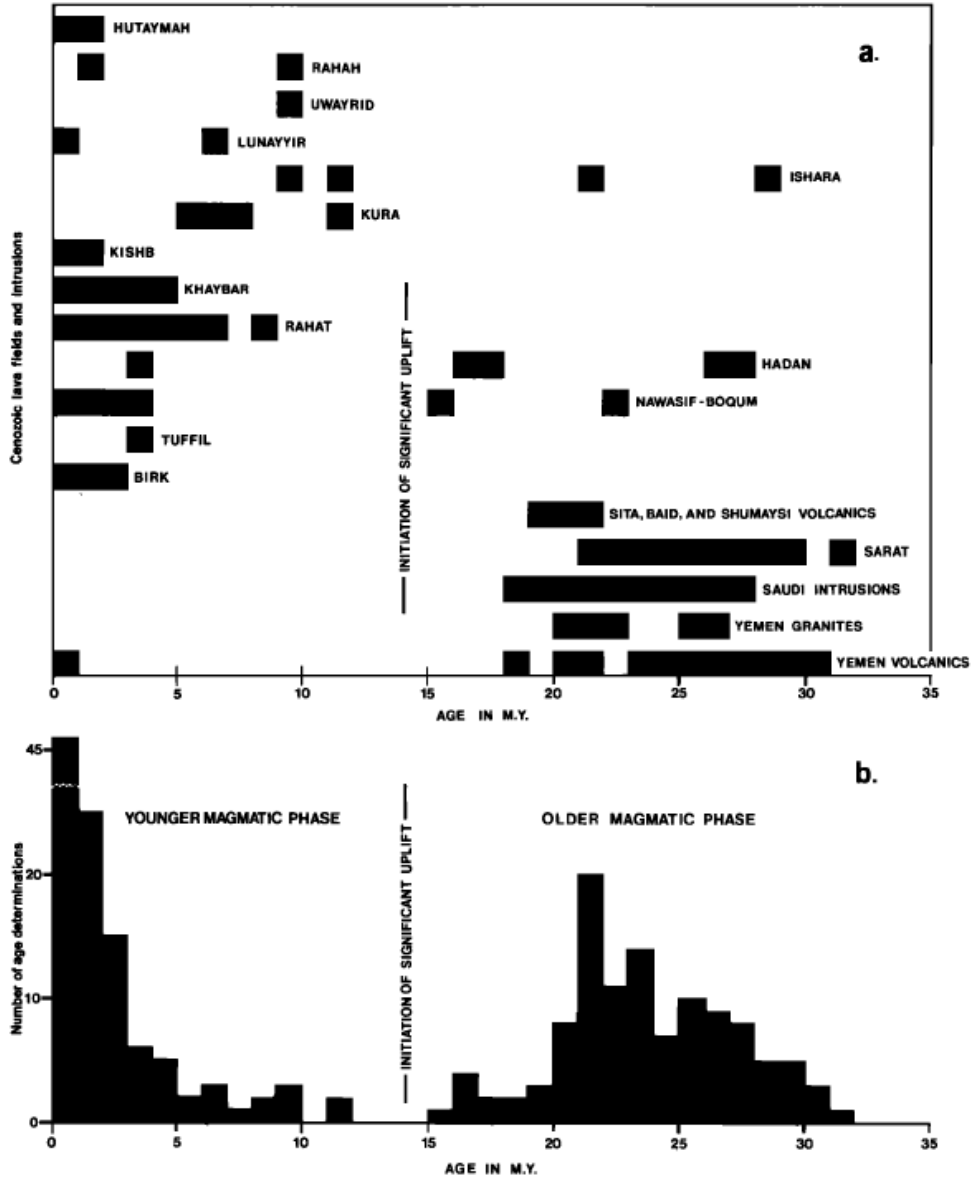


Figure 2. Compilation of radiometric ages for lava fields, intrusions and volcanic interbeds east of the Red Sea in Saudi Arabia (182 determinations) and Yemen (41 determinations). Data summary from Camp and Roobol [1992]. The compilation does not include ages from the northern part of the Arabian continental basalt province beyond the northern latitude of the Red Sea at 28°N; nor does it include those age determinations older than 35 Ma. Most ages here are also based on the less precise and accurate K-Ar technique From [Camp and Roobol \(1992\)](#).

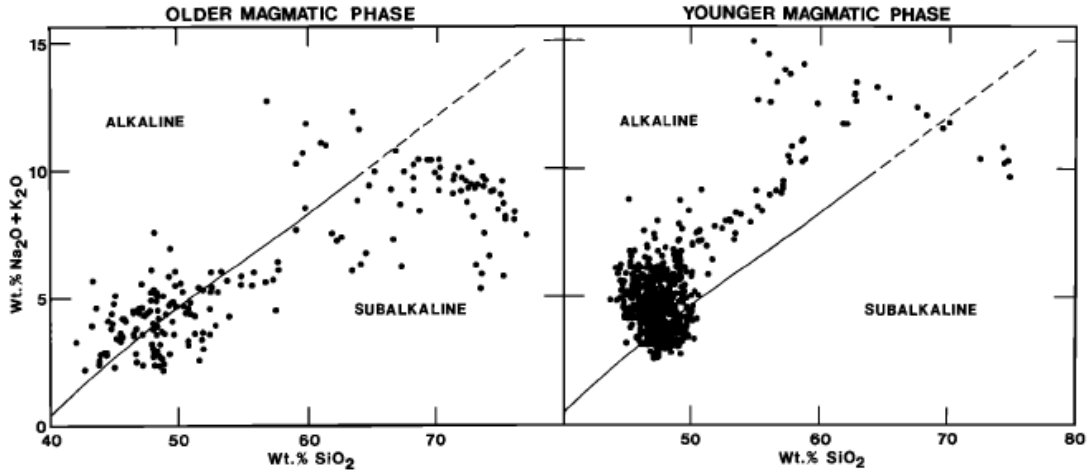


Figure 3. Total alkali versus silica diagram for 742 analyses of the older (30 to 20 Ma) and younger (12 to present) magmatic phases from Yemen, Saudi Arabia, and Jordan. The younger group of harrats can be further divided into mildly alkaline and strongly alkaline lava fields. From [Camp and Roobol \(1992\)](#).

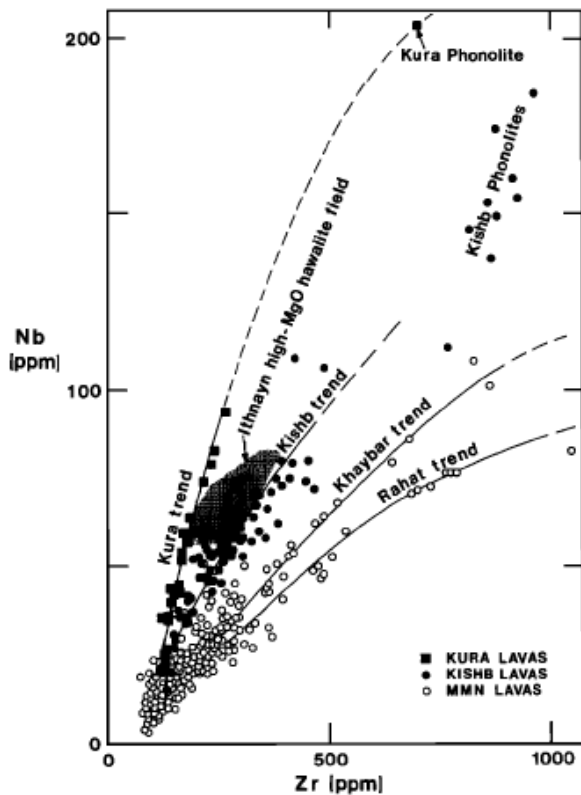


Figure 4. Variation in Zr/Nb for the MMN harrats (Rahat, Khaybar and Ithnayn) and the flanking Harrats Kura and Kishb. The only MMN harrat samples with low Zr/Nb ratios, similar to those from Harrats Kura and Kishb, are a few high-MgO hawaiites located at the northern end of the MMN volcanic line on Harrat Ithnayn (shaded region). From [Camp and Roobol \(1992\)](#).

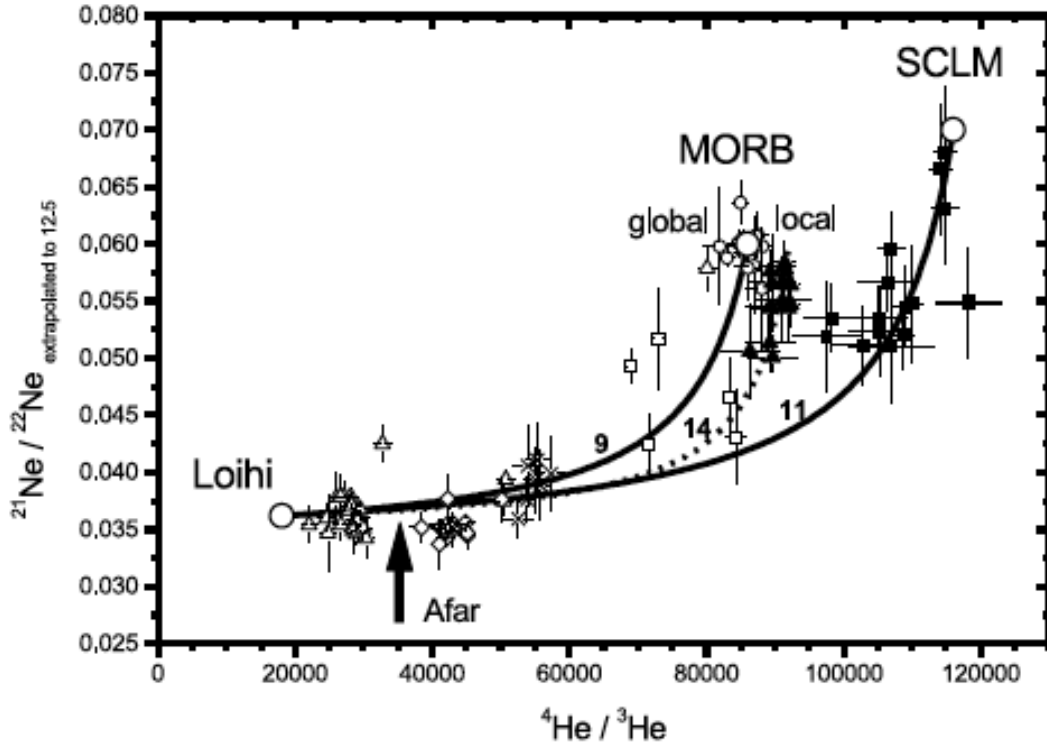


Figure 5. He-Ne isotope systematics. $^{21}\text{Ne}/^{22}\text{Ne}$ ratios extrapolated to a mantle end-member value of $^{20}\text{Ne}/^{22}\text{Ne}=12.5$, plotted against $^4\text{He}/^3\text{He}$ ratios. Two subsets of data from this study are represented by solid squares (5 samples) and solid up triangles (2 samples), the latter more similar to MORB. For comparison, data from mantle plumes like Loihi-Kilauea (Hawaii, open up triangles), Iceland (open diamonds) and Reunion (crosses), normal MORB (open circles) and Red Sea basalt glasses (open squares) are included. Error bars are 1σ . To exclude measurements possibly disturbed by elemental fractionation during gas extraction for analysis, only data of crushed samples and total fusion data of heated samples were used. The calculated mixing lines shown represent two-component mixing between an approximated Loihi-type mantle plume end-member (big open circle, lower left) ($^4\text{He}/^3\text{He}=18,050$ ($40 R_A$), $^{21}\text{Ne}/^{22}\text{Ne}_{\text{Extr}}=0.0362$) and (i) a more radiogenic/nucleogenic sub-continental lithosphere mantle component (big open circle, upper right) ($^4\text{He}/^3\text{He}=116,000$ ($6.2 R_A$), $^{21}\text{Ne}/^{22}\text{Ne}_{\text{Extr}}=0.070$), (ii) a global MORB component (big open circle, upper left) ($^4\text{He}/^3\text{He}=86,000$ ($8.4 R_A$), $^{21}\text{Ne}/^{22}\text{Ne}_{\text{Extr}}=0.060$) and (iii) a possible local MORB component ($^4\text{He}/^3\text{He}=92,000$ ($7.85 R_A$), $^{21}\text{Ne}/^{22}\text{Ne}_{\text{Extr}}=0.060$). The latter mixing trend is distinguished as a dotted line. Numbers indicate the used r-values. The arrow marks the approximate position of the Afar plume (at $20 R_A$). From [Hopp et al. \(2003\)](#).

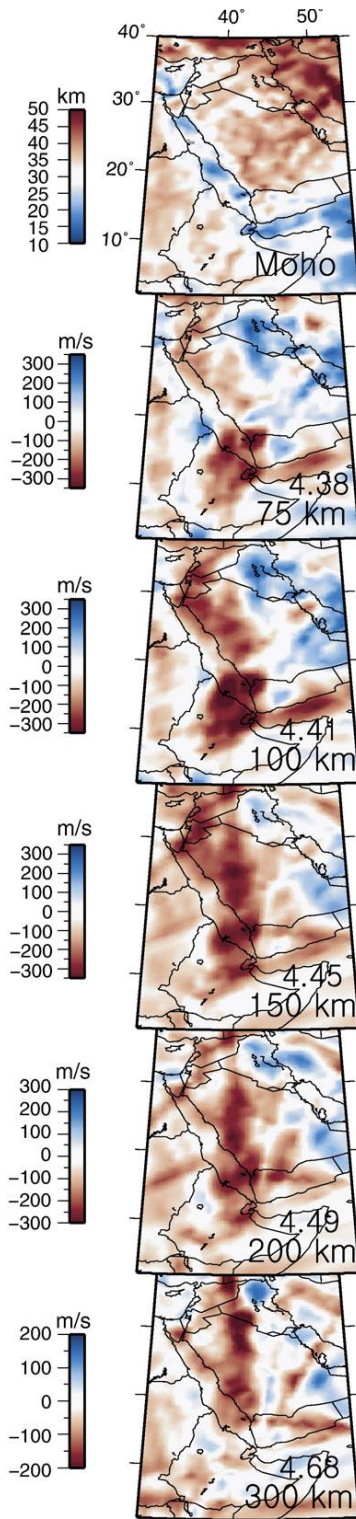


Figure 6. Moho depth and depth slices at 75, 100, 150, 200, 300, 400, 500, 600, 700, 1000, and 1400 km from the joint inversion model (Chang and van der Lee, 2011). Velocity perturbations are relative to the reference model “MEAN” (Marone et al., 2004), and the reference S velocity at each depth is written on the right side in km/s scale. From Chang and van der Lee (2011).

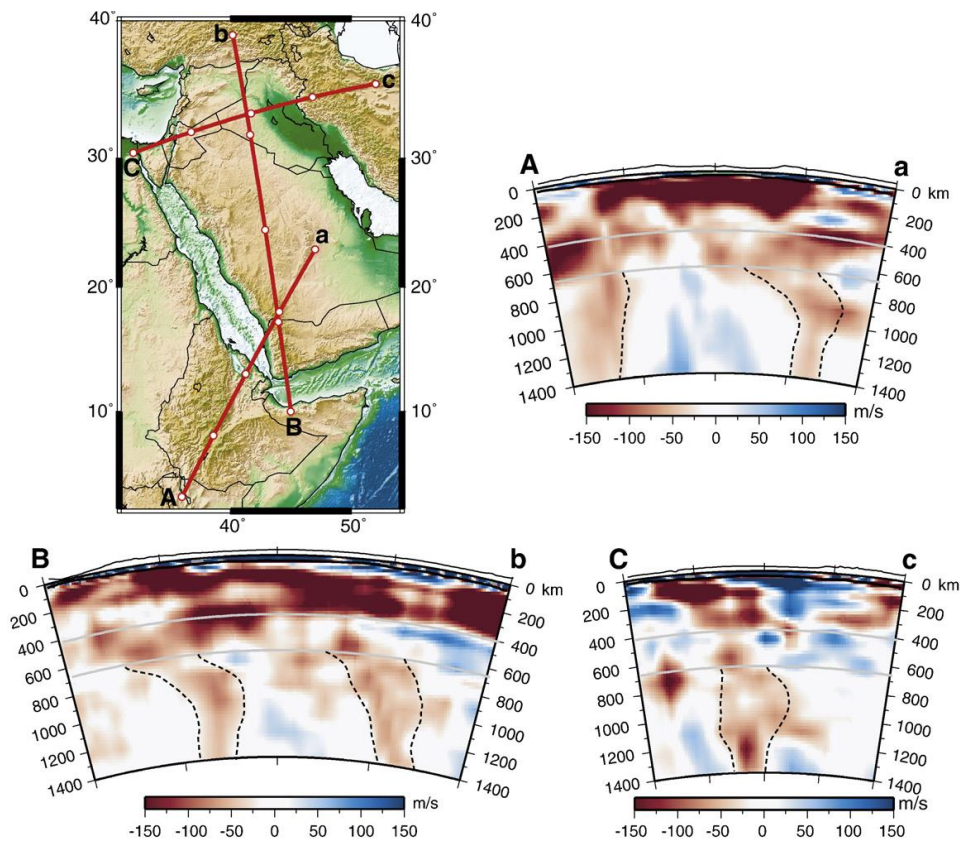


Figure 7. Vertical cross-section maps encompassing Ethiopia and southern Arabia (A-a), across the Arabian Peninsula in approximately N-S direction (B-b), and from the Sinai Peninsula to Iran (C-c). Low-velocity anomalies, which are thought to be mantle plumes, are surrounded by dashed lines. Moho depth and 10 times exaggerated surface topography are indicated by black lines. Gray lines represent discontinuities at 410 and 660 km. Great-circle paths corresponding to cross sections are shown on the left-top map. White circles on the great-circle paths correspond to ticks in the cross sections. From [Chang and van der Lee \(2011\)](#).

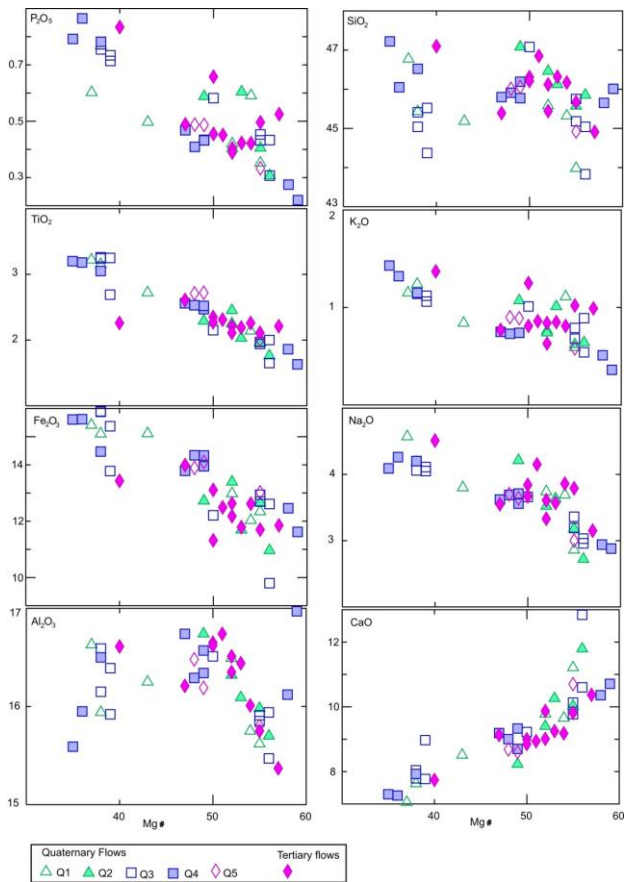


Figure 8. Variation of major and minor elements versus Mg# basalts from Harrat Lunayyir. There is no apparent correlation between phase of volcanic construction and degree of magma evolution. Al-Amri et al. (unpublished data).

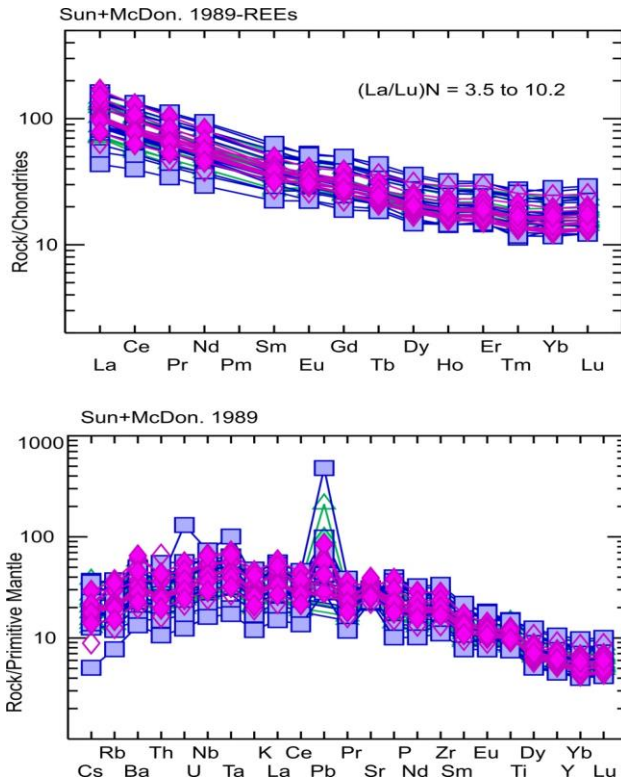


Figure 9. Chondrite-normalized REE patterns (upper) and spider diagrams of trace elements normalized to primitive mantle (lower) for the Harrat Lunayyir rocks. The elements are arranged in order of increasing incompatibility from right to left. Al-Amri et al. (unpublished data).

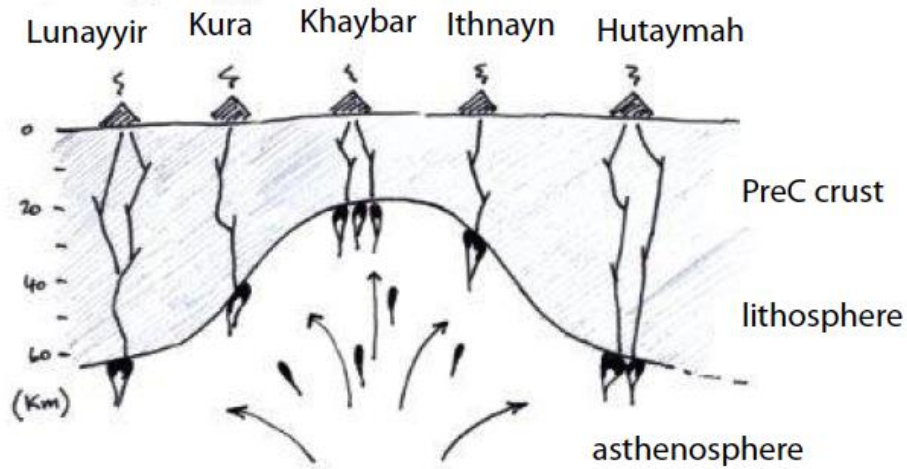


Figure 10. Schematic E-W cross-section through the central western Arabian harrats. Major and trace element data predict that the lithosphere-asthenosphere boundary has shallowed due to thermal erosion (mantle upwelling or horizontal flow?), such that volcanic centers along the MMN line are constructed of magmas formed from greater degrees of partial melting and separation from the mantle at shallower depth than volcanic centers on the margin, constructed of magmas formed from smaller degrees of partial melting and deeper separation from the mantle.

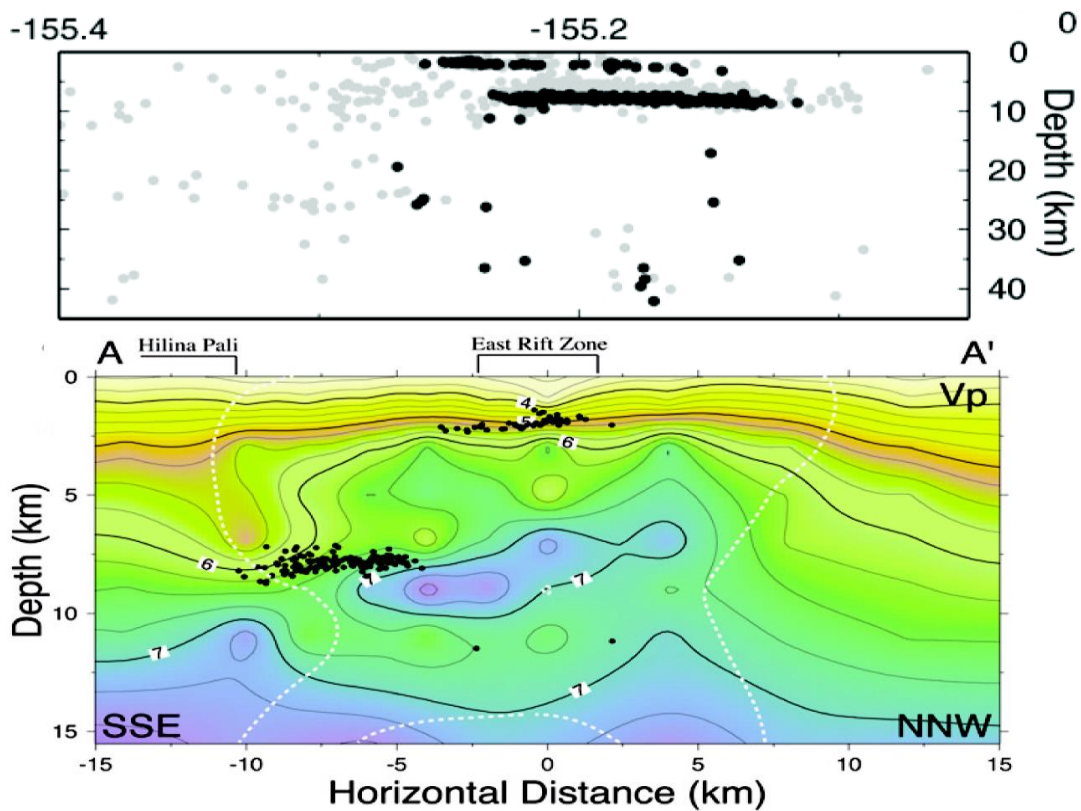


Figure 11. (Top) Initial (gray dots) and final (black dots) earthquake locations and (bottom) P-wave velocity structure beneath the South Flank of Kilauea Volcano, Hawaii, determined using the SIMULPS tomographic inversion method. From [Hansen et al. \(2004\)](#).

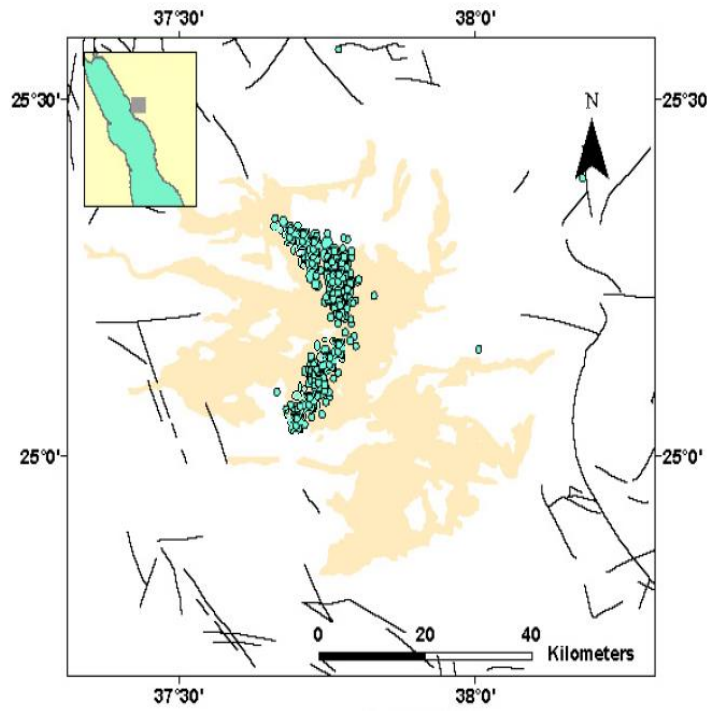


Figure 12. Aftershocks from May 20 to June 19, 2009, within Harrat Lunayyir. Al-Amri et al. (unpublished data).